Postharvest Biology and Technology 219 (2025) 113276

Contents lists available at ScienceDirect

Postharvest Biology and Technology

journal homepage: www.elsevier.com/locate/postharvbio

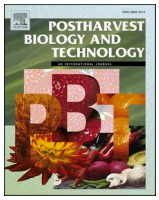

Multiple genetic analyses disclose the QTL dynamic for fruit texture and storability in Norwegian apples (*Malus domestica* Borkh.)

Liv Gilpin [a,*,1], Fabrizio Costa [b,2], Nicholas P. Howard [c], Dag Røen [d], Muath Alsheikh [a,e]

[a] Department of Plant Sciences, Norwegian University of Life Sciences, Ås 1433, Norway
[b] Center of Agriculture Food Environment (C3A), University of Trento, Via Mach 1, San Michele all'Adige, Trento 38098, Italy
[c] Fresh Forward Holding B. V., Hogewoerd 1 C, Huissen 6851 ET, the Netherlands
[d] Njøs Fruit and Berry Centre, Leikanger 6863, Norway
[e] Graminor Breeding Ltd, Ridabu 2322, Norway

ARTICLE INFO

Keywords:
Apple
QTL mapping
GWAS
PBA
Storability
Texture
Fruit breeding

ABSTRACT

In Norway, apples (*Malus domestica* Borkh.) are produced at latitude around 60° north. Notably the season is short and cool and Norwegian cultivars have developed under selection pressure from these distinct climatic conditions, resulting in apple germplasm with unique genetic structure and pedigree. Strong selection for earliness has resulted in several cultivars that mature and soften quickly, making it challenging to meet consumer expectations for apple quality. The commercial success of apple is largely related to its texture and long-term storability, enabling a year-round availability of fresh fruit. Texture in apple has been well characterized and major causative genes have been found. Nonetheless, comprehensive knowledge of the genetic control of texture retention is lacking. To improve postharvest performance, including storability, in the breeding program currently ongoing at Njøs Fruit and Berry Centre (NJØS), a diversity collection of 197 apple cultivars was employed to initiate a genome-wide association analysis (GWAS) to identify relevant genomic regions associated with these aspects. Quantitative trait loci (QTL) associated with different dissected multi-trait texture components assessed by a texture analyzer equipped with an acoustic device were identified. To target QTLs relevant to improving postharvest storage, a softening and storage index was also implemented into the QTL analysis, further mapped on chromosome 10. The GWAS-QTL pattern was additionally validated on a different genetic background, implementing a multi-parental-cross-design scheme. Findings include previously unreported genomic regions related to texture attributes, and especially haploblock HB-10–03 represents an important novel molecular tool valuable for breeding Norwegian apple cultivars with superior fruit storability.

1. Introduction

Apples (*Malus domestica* Borkh.) are grown in southwest and eastern Norway, around latitude 60° north. The growing seasons in these regions are cooler and shorter (1211–1775 growing degree days, 168–195 days) and have longer days in the summer than other European fruit-growing areas (Ikase, 2015). Since the 11th century (Oye, 1998), Norwegian heirloom cultivars were developed under selection pressure from these distinct climatic conditions and from cultural preferences of local farming communities. In a recent study, the genetic structure and pedigree of Norwegian heirloom cultivars were clearly distinguished from North American, Asian, and European cultivars (Gilpin et al., 2023). The climatic conditions in the Norwegian apple growing regions demand careful selection of adapted cultivars, with earliness and winter hardiness being the main limiting factors (Ikase, 2015). Earliness has always been an important goal in the Norwegian Apple Breeding Program (NABP). Early-maturing cultivars, however, have been reported to soften fast, making it challenging to meet modern-day consumer expectations for apple quality. While apple cultivars historically were appreciated primarily for their taste attributes, consumers now rate firmness and crispness as paramount quality features (Bowen et al., 2019).

* Correspondence to: Norwegian University of Life Sciences, Elizabeth, Stephansens v. 15, Ås 1433, Norway.
E-mail addresses: liv@njos.no (L. Gilpin), fabrizio.costa@unitn.it (F. Costa), Nick.Howard@fresh-forward.nl (N.P. Howard), dag@njos.no (D. Røen), muath.alsheikh@graminor.no (M. Alsheikh).
[1] https://orcid.org/0000-0003-2587-7450
[2] https://orcid.org/0000-0003-1416-1078

https://doi.org/10.1016/j.postharvbio.2024.113276

Besides fruit quality appreciation, fruit texture is also important for the maintenance of fruit quality and nutritional content during storage. Fruit storage potential is an important trait for marketability (El-Ramady et al., 2015; Nybom et al., 2010). Apple fruit storability largely depends on the type of texture, which relies on the dismantling process occurring within the cell wall/middle lamella polysaccharide structure operated by a genetically coordinated action of several cell wall degrading enzymes. There is a great variability of polysaccharidic architecture modification in apple, leading to textures ranging from mealy to crispy (Galvez-Lopez et al., 2011). Storability is therefore a dynamic aspect, related to the loss of textural properties over time, rather than a static assessment carried out at a specific physiological time point.

The genetic control of texture retention, and particularly crispness retention, in apple is still not fully elucidated, and it has not been previously studied in any Norwegian germplasm. Besides consumer appreciation, a favorable texture and a slow softening also prevent fruit decay and development of important postharvest disorders and diseases, thus strengthening food security and decreasing the need for imports at a time when 83.5 % of the apples consumed in Norway are currently imported from other apple producing countries (OFG, 2024). Apple texture is well characterized and recognized as a sensory property consisting of several parameters, largely grouping into two components, mechanical, and acoustic, valuable to describe firm and/or crisp apples, respectively (Costa et al., 2012). Major Quantitative trait loci (QTL) associated with mechanical and acoustic components of apple texture have been detected on chromosome 10 via several genetic approaches, such as pedigree-based analyses (PBA), genome-wide association analysis (GWAS), and pseudo-test cross based strategies (bi-parental families) (Costa et al., 2010; Di Guardo et al., 2017; Farneti et al., 2017). These QTLs coincided with the polygalacturonase gene *MdPG1* (Longhi et al., 2013). Other QTL regions for texture have been identified on other genomic positions, such as chromosomes 10, 15, and 1, and collocating with *MdACO1*, *MdACS1,* and *Md-Exp7*, respectively, which are other important genes controlling fruit ripening and texture (Costa et al., 2005; Costa et al., 2008). Recently, another gene, *NAC18.1*, was located within a QTL region on chromosome 3 and associated with the control of fruit firmness at harvest (Migicovsky et al., 2021). These studies have been useful to decipher the genetic control of fruit texture at harvest or after a period of storage, however storability was not considered. Up to now, firmness at harvest has been the most commonly investigated parameter in previous studies on texture in apple (Nybom, 2023).

In this work, our goal was to identify the most important genomic regions controlling the variation in fruit texture, including both firmness and crispness, among Norwegian cultivars, and to find potential SNP markers suitable to assist the selection processes of the NABP. The validation of QTLs identified within the NAAC using the GWAS strategy was performed by using the PBA approach on five biparental mapping populations related by pedigree.

2. Materials and methods

2.1. Plant material

For this study, 197 apple accessions (Table S1) were chosen to constitute the NAAC collection, including diploid Norwegian heritage cultivars, recent international releases, NABP cultivars and selections, all available at NJØS (at latitude 61° 10'43.2" N, longitude 6°51'34.3" E), located at the Sognefjord, western Norway. A minimum of two trees per accession were planted between 2014 and 2016 in a nonreplicated design. The SNP-trait association validation panel was represented by five biparental populations generated by crossing different accessions with known variation in texture attributes, all included in the NAAC collection and planted between 2016 and 2018 (Table S2). Trees in NAAC were maintained with standard agronomic practices for fruit thinning, pruning, and pest/disease control, and trees in biparental populations were only sprayed to control the apple proliferation phytoplasma vector *Cacopsylla melanoneura*.

2.2. Phenotypic assessment

Phenotypic data were collected in 2022 for GWAS and in 2023 for validation of SNP-trait associations in biparental populations. The apples were harvested at a defined ripening stage determined by the degradation of chlorophyll content assessed nondestructively with a DA meter (TR turoni, Forli, Italy) as described in Farneti et al. (2017) and Busatto et al. (2016). Fruit was regularly monitored with the DA meter at two opposite sides of the equatorial area for the correct harvest date, defined with threshold means between 0.8 and 1 on two technical and ten biological replicas. For each apple accession, a minimum of 24 homogeneous apples were collected and stored for two months at room atmosphere (3 °C with ~95 % relative humidity). Ten apples were evaluated at each time point (harvest and postharvest) and four additional apples were collected as backup in case of storage loss. Apples were carefully harvested from well-exposed areas of the tree, avoiding the top and the bottom of the canopy. Cracked, rotten or otherwise quality-degraded fruit was avoided if possible. For texture analysis, fruit samples excluding peel and core, were prepared into discs following the method described by Costa et al. (2011). Fruit crispness and firmness were estimated both at harvest and after postharvest storage by the TAXT plus computer-controlled texture analyzer (Stable Micro System, Godalming, UK) equipped with an acoustic envelope detector (Laurens et al., 2018). Instrumental measurements followed the protocol described in Costa et al. (2011). For each genotype, 25 measurements (five technical per five biological replicates) were carried out. Mechanical and acoustic profiles were further processed with an ad hoc macro developed by Costa et al. (2011) for the digital definition of nine parameters. Of these (Table S3), six were related to the mechanical signature of texture ("yield force" (YF), "maximum force" (MF), "final force" (FF), "force linear distance" (FLD), "Young's Modulus" (YM), and "number of force peaks" (NFP)) while the other three were related to the acoustic response ("maximum acoustic pressure" (MXA), "mean acoustic pressure" (MEA), and "number of acoustic peaks" (NAP)) as described in Costa et al. (2011). Data obtained at harvest and postharvest together with the storage index, were used to plot the distribution of the 197 accessions from the NAAC using principal component analysis (PCA), performed and visualized with the statistical software R version 4.3.0 (R Core Team, 2023) and the package FactoExtra (Kassambara & Mundt, 2017). Mechanical and acoustic signatures of fruit texture were assessed at harvest, after two months of postharvest storage, and via a softening and a storage index parameter (described below) to examine the behaviors of each texture property during storage. Data related to parameters computed here were standardized by means. Variance in texture attributes among the accessions were investigated using PCA, and illustrated in a single bidimensional plot. To investigate dependence between multiple variables simultaneously, a correlation matrix was computed with R package Hmisc (Harrell Jr & Harrell Jr, 2019) using the Pearson correlation coefficient and significance level 0.01.

2.3. Dynamic aspects of fruit texture

To evaluate the degree of softening and storability, defined as the change of each dissected texture parameter measured in this study, the storage index presented in Costa et al. (2012) and the softening index, were computed for each accession. The softening index was calculated as the difference between texture parameter values acquired at harvest and after storage. The storage index (*SI*) was instead computed as

$$SI = \log_2\left(\frac{\mathrm{T}i\mathrm{P}}{\mathrm{T}i\mathrm{H}}\right)$$

where T_iH is the mean value of "*i*" texture (T) parameter measured at

harvest (H), and T_iP is the mean value of the same texture parameter measured after storage (P). Positive storage index values indicated a texture enhancement for the respective texture parameter, while negative values pointed to a loss of textural performance during storage. A value equal to zero meant stable maintenance of respective textural traits during storage. The storage index was calculated for each of the twelve texture parameters across 197 accessions and a PCA was performed to estimate an overall measurement of storage potential.

2.4. Genotype data

SNP genotyping was conducted using the 20 K Infinium® apple SNP array (Illumina Inc., San Diego, USA) (Bianco et al., 2014) and SNP data was curated as described in Vanderzande et al. (2019). Only SNPs included in the set of robust SNPs presented in Howard et al. (2021) were kept, resulting in 10,321 SNPs remaining for downstream analysis. Population structure was used as a cofactor in GWAS, using the findings from the structural analyses in Gilpin et al. (2023). For SNP data curation, as well as subsequent QTL mapping, genetic positions were taken from an updated version of the integrated genetic linkage map (Di Pierro et al., 2016) as described in Howard et al. (2017). All pedigree relationships employed in this study have been validated through SNP data using the process described in Howard et al. (2021) to confirm the ancestors of 'Honeycrisp'.

2.5. GWAS on texture traits

GWAS was performed for each recorded trait assessed on the 197 accessions of the NAAC collection (Table S1). Each texture parameter, together with the two principal components (Dim1 and Dim2, used to resolve redundant variables), were considered phenotypic data and employed in the association study to identify QTLs associated with apple fruit texture. GWAS was performed with four different mixed linear models (MLM, MLMM, ECMLM, and FarmCPU) implemented in the GAPIT software version 3 (Wang & Zhang, 2021) and tested for consistency. Furthermore, different covariates to account for population structure and a given number of principal components depending on trait were tested. Different multiple comparison adjustments, both Bonferroni (Holm, 1979) corrections at $\alpha = 0.01$ and $\alpha = 0.05$ and FDR (Benjamini & Hochberg, 1995) at 5 % and 10 %, were compared. Additionally, the shape of peaks in the Manhattan plots and the number of associated SNPs forming the peaks, as well as MAFs of those markers, were considered when determining the reliability. MLM and ECMLM are single locus models and can introduce false negatives due to over fitting of the model (Kaler et al., 2020), hence only trait-SNP associations from MLMM and FarmCPU were finally considered. The FarmCPU model uses MLMM and incorporates multiple markers simultaneously as covariates to partially remove the confounding effects between testing markers and kinship. Finally, significant differences among allelic configurations for each important QTL for the associated phenotypic trait were tested through analysis of variance (ANOVA). Genes in the region of a significant SNP marker were explored using the Genome Database for *Rosaceae* (GDR) website available at www.rosaceae.org (Jung et al., 2019) for the GDDH13 v1.1 reference genome (Daccord et al., 2017).

For assessing QTL detection pattern for texture properties across harvest, postharvest, and the storage index, three representative texture parameters, YF, NAP, and NFP were selected. The YF defines the point of transition from the elastic to the plastic phase of the mechanical profile, while both NFP and NAP identify the number of ruptured cellular events simultaneously acquired by both mechanical and acoustic profiles.

2.6. QTL discovery using a pedigree-based approach

PBA was performed using FlexQTL™ and VisualFlexQTL software, which implement pedigree-based QTL analysis using a Bayesian approach via Markov Chain Monte Carlo (MCMC) simulations (Bink et al., 2014). The phenotypic entities were represented by each single texture dissected component and Dim1 as defined by the PCA analysis (Table S2). For computational efficiency, nonsegregating markers in the biparental families were removed, resulting in 9572 SNPs. To reduce computation time and optimize visualization of results, curated markers were converted into 545 haploblock(HB) marker sets covering at most 2.00 cM using FlexQTL (Bink et al., 2008) for phasing, VisualFlexQTL (www.flexqtl.nl) and Excel for HB sizing, PediHaplotyper (Voorrips et al., 2016) for haplotype assignment, and again FlexQTL™ for final marker consistency checks. In the analyses, additive genetic models with normal prior distributions and random covariance matrix diagonals were used with 500,000 iterations and a thinning of 500. Distorted marker segregation was allowed through the parameter settings MSegDelta = 1. To confirm identified QTL and their positions, two additional QTL analyses were performed. The maximum number of QTL was set to 10 for all runs, yet different starting seed numbers. The analyses were performed in a genome-wide mode, with a visual inspection of the trace plots after each run until convergence was reached (i.e., the effective chain size exceeded 100) (Sorensen & Gianola, 2002). QTL positions were recorded as QTL intensity estimates via posterior distributions of QTL locations as described in (Sillanpää & Arjas, 1999). Positive, strong and decisive evidence for the presence of QTL was considered when 2*ln Bayes factors (2ln(BF)) (Kass & Raftery, 1995) were greater than two, five and ten, respectively. Additionally, the QTL-biallelic genotype was considered and calculated by FlexQTL with the Q-allele denoting increasing effects and the q-allele denoting decreasing effects on the phenotype. The QTL genotype of each accession included in the pedigree was a priori unknown, and alleles were assigned by FlexQTL to founders tracing their transmission to offspring. QTLs were recorded as the median cM value from the MCMC simulation samples within the QTL regions.

2.7. Phenotypic variance explained by harvest date and texture related markers

To decide the proportion of phenotypic variance explained by the texture related markers such as MdACO1, MdACS1, MdPG1, and NAC18.1 and SNP markers identified in this study, a type 2 ANOVA from the 'car' package in R (Weisberg, 2019) was used. A type 2 ANOVA including the markers and harvest date as factors was also performed, to determine the phenotypic variance explained by each marker after accounting for harvest date. Harvest date was quantified using the Growing Degree Hours (GDH) model as presented in Anderson et al. (1986) based on the period between the identified start of active growth and the harvest date. GDH was calculated using hourly temperature data obtained from Landbruksmeteorologisk tjeneste (LMT) weather station located at NJØS, close to the locations where phenotype data were collected. The GDH model considers temperatures between 4 °C and 25 °C as contributing to active growth. Furthermore, we determined the association between harvest date and each phenotype measured (texture at harvest, postharvest and for the storage index) using the Pearson correlation coefficient of each pair of variables, as implemented in the "pairs" function in R (R Core Team, 2023). We visualized the results using the "geom_boxplot" function in the R package ggplot2 (Wickham, 2016).

3. Results

3.1. Principal component analyses

The texture data represented by the mechanical and acoustic profiles with their derived digital parameters collected from the individuals included in the NAAC collection (Table S1), were analyzed through the multivariate statistical approach of principal component analysis that clustered the several parameters into two main groups. The first group was defined by six mechanical parameters, while the second group was

defined by three acoustic parameters (Fig. 1). The apple accessions were evenly spread over the PCA plot defined by the first two principal components PC1 (Dim1) and PC2 (Dim2), together accounting for 83.7 %, 86.5 %, and 74.2 % of the total variability at harvest, postharvest, and for the storage index, respectively. Little clustering originating from genetic structure was observed in the distribution of the accessions based on phenotypic trait variability (Figure S1).

The distribution of each single accession was determined by the loading projection of each variable. At harvest, the texture parameters were separated into three main groups. The first group, located in Quadrant I, included all the acoustic parameters (Table S2), such as MXA, MEA, and NAP, together with the mechanical parameter NFP. In the PCA Quadrant II, two clusters of texture components were observed, the first represented by YM and FLD, the second included FF, MF, and YF (Fig. 1 A). At postharvest, the acoustic parameters with NFP were instead projected towards Quadrant I, while all mechanical parameters were projected in Quadrant II (Fig. 1B). For the storage index (Fig. 1 C), correlations between texture parameters were inconsistent with the two static aspects of fruit texture (harvest and postharvest). In Quadrant I, YF was projected together with MF, FF, and YM. In Quadrant II, MXA and MEA were instead projected with FLD. Moreover, between these two groups, another cluster including NFP, NAP and YM was also observed. In all the three projections of texture variables, depicted in the three PCA plots (Fig. 1), the Dim1, accounting for a variability of 48.8 % at harvest, 73.6 % at postharvest, and 57.1 % for the storage index, was related to the general behavior of texture. The Dim2, although representing a minor variability (34.9 % at harvest, 12.7 % at postharvest, and 17.1 % for the storage index), specifically distinguished acoustic from mechanical components (Table S4).

The relationship among the parameters were furthermore confirmed in a correlation matrix (Figure S2). The main mechanical parameters YF, FF, and MF were significantly correlated (0.95 – 0.99) at all stages, yet FLD and YM were less correlated with the other mechanical parameters (0.43 – 0.94). The set of acoustic parameters, MXA, MEA, and NAP, together with the mechanical parameter NFP, showed a correlation ranging from 0.64 to 0.79. The sets of mechanical and acoustic parameters were only partially correlated (0.50 – 0.76) when assessed after storage, yet not correlated (-0.08 – 0.05) at harvest.

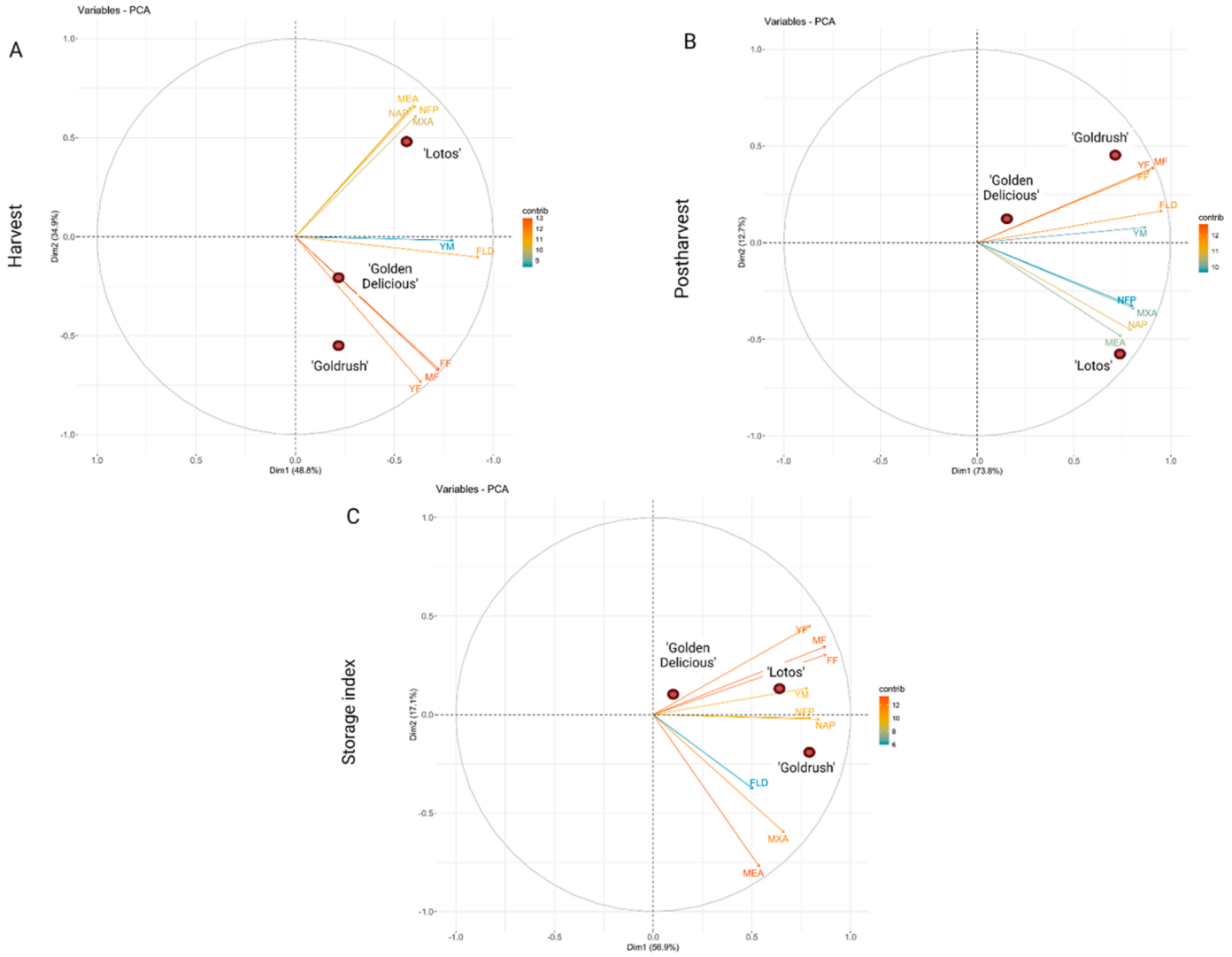

Fig. 1. Two dimensional PCA plots of variables illustrating the fruit texture variability evaluated in the NAAC, at harvest (A), postharvest (B) and for the storage index (C). For the loading variables (Table S3), yield force (YF), maximum force (MF), final force (FF), force linear distance (FLD), Young's Modulus (YM), number of force peaks (NFP), maximum acoustic pressure (MXA), mean acoustic pressure (MEA), and number of acoustic peaks (NAP), their contribution to the overall variance is highlighted with coloration according to the depicted scale. In Table S4 are the contributions of variables in accounting for the variability in Dim1 and Dim2 expressed in percentage. In each PCA plot, the position of 'Golden Delicious', 'Lotos' and 'Goldrush' is highlighted.

3.2. A genome-wide scan identifies major QTL associated with specific texture parameters

A GWAS approach was carried out to identify QTLs associated with apple texture properties, and the visual inspection of Q-Q plots between the two selected models, MLMM and FarmCPU, revealed that FarmCPU was more reliable in the control of both false positives and negatives. The overall GWAS identified a series of SNPs associated with six mechanical (NFP, YF, MF, FF, FLD and YM) and three acoustic parameters (NAP, MXA, and MEA), together with Dim1. The associated SNPs were distributed over all 17 chromosomes (Table S5). Among the texture parameters, FF and NAP showed the highest numbers of SNP-trait associations, respectively. On chromosome 1, significant associations for the mechanical traits (FLD, MF, and YF) at position 19,185,268 bp (based on the GDDH13v1.1 genome) were found, with a value ranging from 6.7 to 9.0 $-\log_{10}(P)$. On chromosome 3, the SNP_FB_1118253 was found significantly associated with the mechanical trait LDF and the acoustic parameter MXA, located at 33,202,503 bp with 6.7–9.0 $-\log_{10}(P)$. On chromosome 5, QTLs were found associated with three mechanical traits (YF, MF, and FLD) at 15,280,685 bp. Other SNP-texture parameter associations were found on chromosomes 7, 11, 12, and 15 (Table S5).

Chromosome 10 showed the highest number of SNPs associated with texture components, located in two specific genomic regions. The first region (located in a range of 3022,149—3685,125 bp) included SNPs with $-\log_{10}(P)$ from 4.3 to 6.0, while in the second region (identified at 23,555,573—36,547,260 bp) SNPs with $-\log_{10}(P)$ from 4.6 to 7.4 were identified. For the acoustic traits, reliable associations were detected in the same genomic regions, located between 2975,006—3685,125 bp (5.8—5.9 $-\log_{10}(P)$) and between 2975,006—3685,125 bp (5.8—5.9 $-\log_{10}(P)$). For the overall texture storability (Dim1 storage index), the GWAS identified two QTL regions on chromosome 10 (Fig. 2), with the first QTL region having four markers exceeding the false discovery rate (FDR) corrected *p*-value threshold. The most significant SNP ("SNP_FB_0003490") identified was located at 3685,125 bp on the GDDH13v1.1 whole genome sequence (Daccord et al., 2017). The second region associated with Dim1 was instead detected both after storage and for the storage index (Figs. 2B and 2 C), at 23,602,458 bp downstream from the first identified QTL region, exceeding the FDR corrected *p*-value threshold only at postharvest. The variability of the "SNP_FB_0003490" marker (Fig. 3 A) was used to differentiate the distribution of Dim1 storage index according to diplotype (Fig. 3B). Based on statistical analysis carried out among three possible diplotype categories, only a double dose of the favorable "C" allele showed a significant difference with respect to the other two ("AA" and "AC").

The in silico gene mining and annotation identified three important gene families, all involved in the metabolism of the cell wall polysaccharidic architectural structure, for the most significant GWAS hit on chromosome 10, namely an *endoglucanase* gene (MD10G1006400), two *xylan alpha-glucuronosyl transferase* genes (MD10G1015800, MD10G1015900) and a *cellulose synthase* (MD10G1029800) gene.

3.3. QTL dynamics for fruit texture

The comparison of the combined mechanical and acoustic profiles of texture assessed for all the accessions included in the NAAC collection at harvest and after storage, enabled the definition of texture dynamic patterns, such as type I (represented by 'Golden Delicious'), type II (represented by 'Goldrush'), and type III (represented by 'Lotos') (Fig. 4). In type I texture dynamics, a general loss in performance was detected for both mechanical and acoustic profiles during storage. Meanwhile, in type II dynamics, a decline only in acoustic performance was observed, while the mechanical performance remained substantially unchanged. The last texture dynamics scenario, type III, was characterized by an opposite behavior in respect to type II, with a considerable reduction in the mechanical performance while the acoustic displacement after storage remained at the same level as assessed at harvest (Fig. 4). Most of the associations, regardless of their genomic positions, were detected for textural performance at postharvest (Table S5), as exemplified by the QTL results obtained for Dim1 that differed significantly according to the phenotyping time points (Fig. 2). For the fruit texture assessed at harvest (Fig. 2 A), no clear associations were detected, while after storage (Fig. 2B), or for the storage index parameter (Fig. 2 C), an increased magnitude in the association level was detected around a locus specifically located on chromosome 10.

The number of QTLs detected corresponded with the magnitude of phenotypic variability for each specific trait. This was exemplified with the three sub-traits, YF (mechanical attribute), NFP (mechanical attribute correlated to acoustic attributes), and NAP (acoustic attribute) as shown in Fig. 5 for the association computed with the MLMM model at both the harvest and postharvest time point. For the two dynamic aspects of fruit texture (softening and storage index), similar results were consistently obtained, hence the one with the most significant results was chosen. YF had a reduction of phenotypic variance when the softening index was used as a parameter, which lead to a reduced magnitude in the GWAS, and consequently, no associated SNPs were identified. The other two textural parameters showed, instead, an increasing variance after storage, with a twofold increase for NAP (Fig. 5). For these two parameters, no QTLs were detected at harvest, while for NFP, two QTLs were identified when the softening index was used as phenotypic entity (Table S6). For NAP, a total of three QTLs were identified, two after storage and one for the softening index (Table S6). The QTL for the softening index was detected on chromosome 10, corresponding to the "SNP_FB_0003490" marker for both NAP and NFP.

3.4. QTL validation through a PBA approach

The initial set of QTLs identified through the GWAS approach was further validated in a set of five half-sib families related by a common pedigree scheme and analyzed employing a PBA approach (Table S2). For the selection of families to be included in the PBA approach, parents with known variation in allelic configuration for texture related markers including the most significant GWAS markers for texture retention were chosen, to further exploit the segregation of these textural aspects. Single markers from the GWAS were converted into haploblocks and the one including "SNP_FB_0003490" (named HB-10–3) was characterized by 13 haplotypes and mapped between 6.79 cM and 12.38 cM (Fig. 3 C). A considerable phenotypic variation could be observed across haplotypes, and the storage index medians of four haplotypes (HT10, HT16, HT24, and HT38) were consistently above zero, corresponding to good storability performance (Fig. 3 C). Among the parents used for QTL mapping, 'X 4876' had the HT10 and HT38 haplotypes, while the cultivar 'Fonn' was heterozygous for the HT24 haplotype.

QTLs were identified and mapped over five chromosomes (Table S7, Figure S3), on which posterior QTL intensity exceeded the posterior probability threshold [$2\ln(BF) > 2$]. Genomic regions with positive evidence ($2\ln BF > 2$) for the presence of QTLs were located on chromosomes 1, 3, 5, 10 and 11 (Table S7). For the two groups of texture-related parameters, distinct QTL probability patterns were obtained (Table S7, Figure S3). Chromosomes 5 and 10 showed QTLs commonly shared by both acoustic and mechanical parameters (Figure S3, Table S7). For the acoustic sub-traits, only MEA had consistently positive evidence of QTLs, which were suggested on chromosomes 5 and 10, with modes at 79.00 cM and 74.00 cM, respectively. Suggested QTLs for the mechanical sub-traits, were mapped on chromosome 5 [$2\ln(BF)_{1/0} = 6.5$—30.9] and 10 [$2\ln(BF)_{1/0} = 2.0$], with a mode at 76.00—78.00 cM and 25.00 cM, respectively. Specifically, for the mechanical sub-trait YM, two additional QTL regions were detected at the center of chromosome 3 and at the end of chromosome 11. A QTL region for the Dim1 computed for the storage index at the end of chromosome 1 was also identified.

For Dim1, when using the storage index parameter, positive evidence

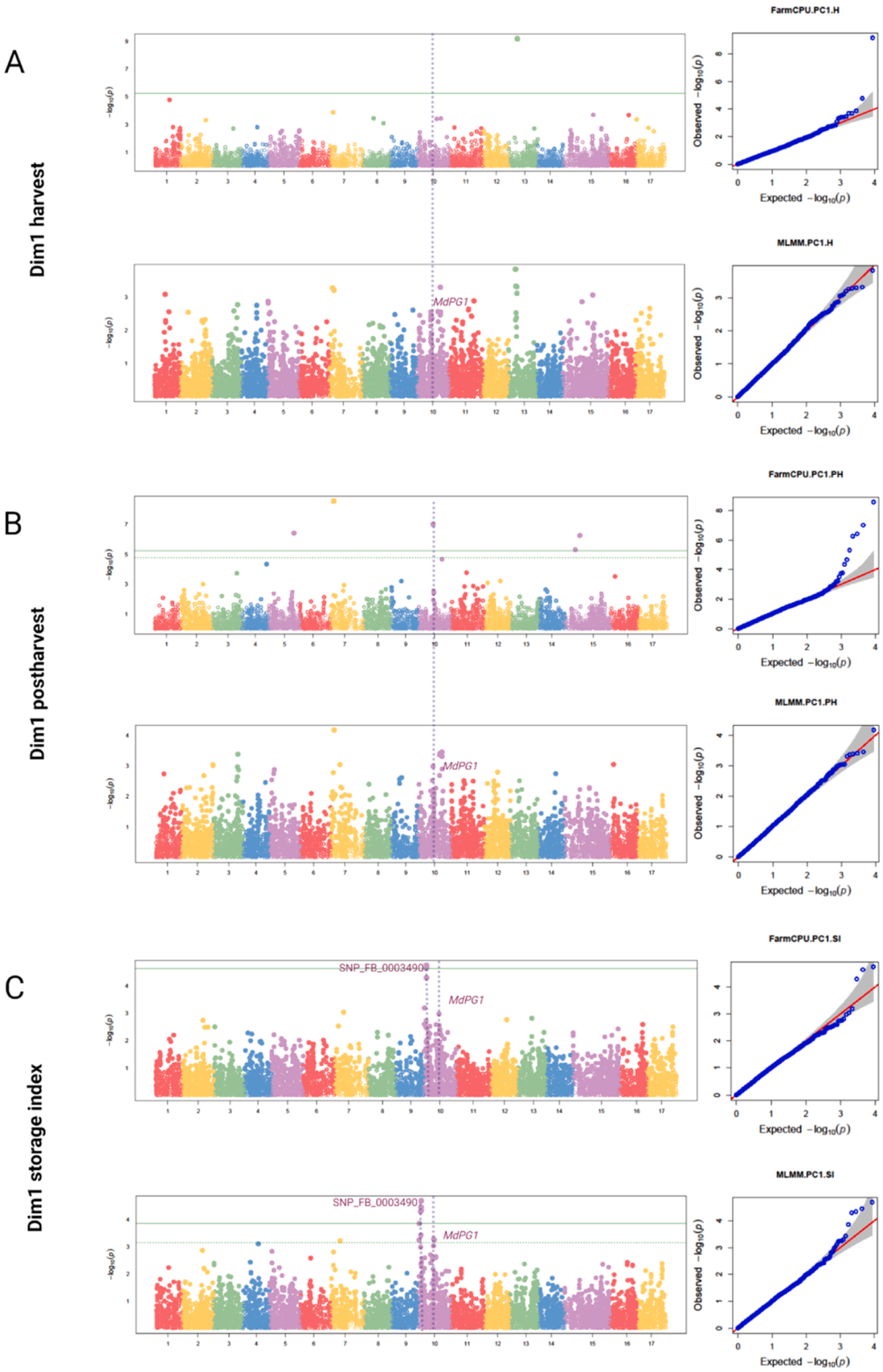

Fig. 2. Manhattan plots using FarmCPU and a mixed linear model with a minor allele frequency ≥5 % and false discovery rate (FDR) corrected significance thresholds of 0.1 and their respective quantile-quantile plots. **A** Dim1 at harvest, **B** Dim1 after two months of cold storage, and **C** for the Dim1 storage index. The position of the MdPG1 gene, next to the strongest signals on chromosome 10 (6.07 cM – 7.08 cM), is depicted in the Manhattan plot of the Dim1 storage index.

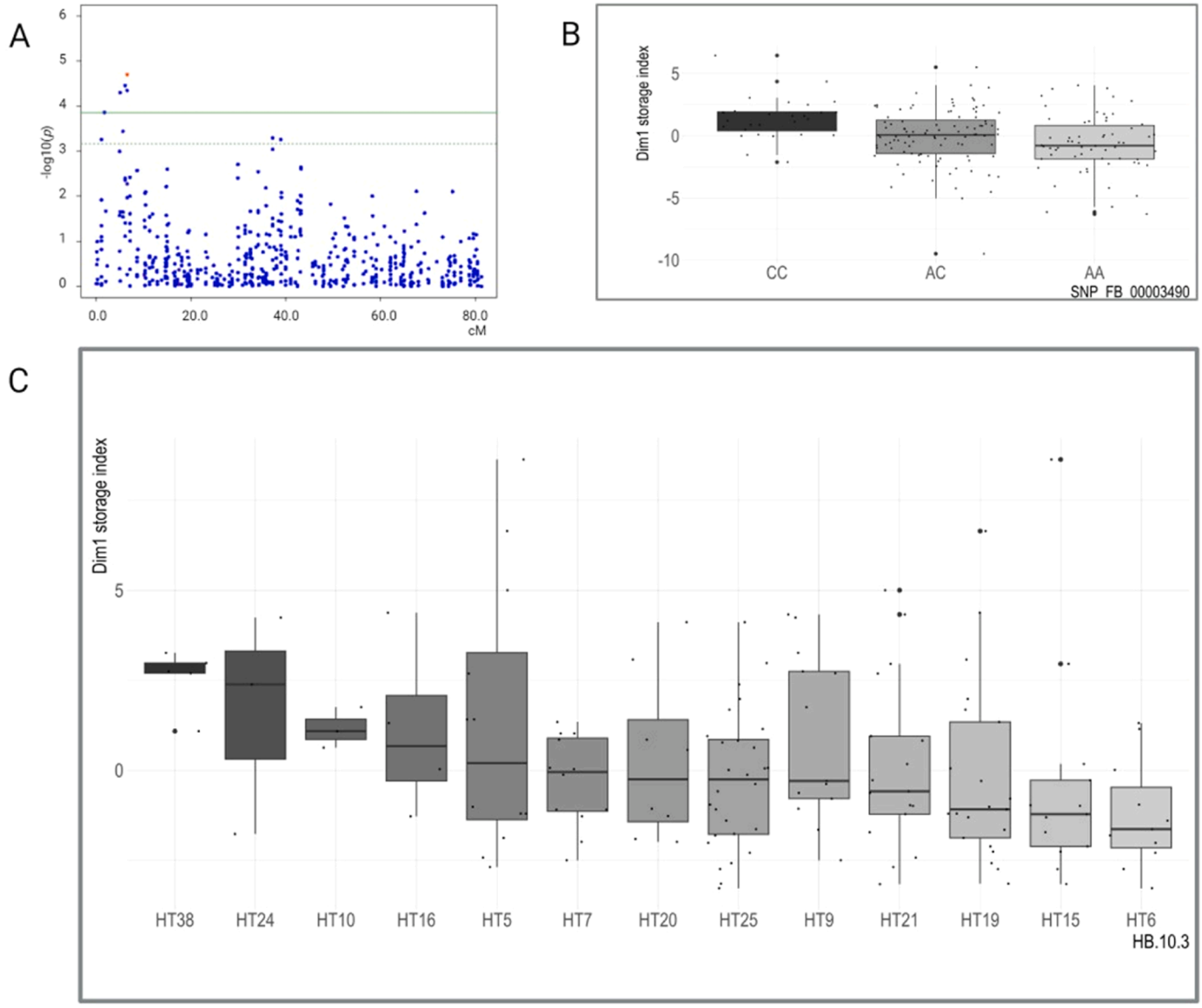

Fig. 3. A SNP associations pattern for the Dim1 storage index for chromosome 10, where SNPs with the highest significance were located, with the most significant marker ("SNP_FB_0003490") marked in red. B Phenotypic distribution of the "SNP_FB_0003490" for the Dim 1 storage index among 197 apple accessions grouped according to their genotype. Different lowercase letters represent significant differences, using Tukey's multiple comparisons of means at 95 % family wise confidence level between homozygous and heterozygous alleles. Positive storage index values indicate texture enhancement, meaning A is the unfavorable allele. C Phenotypic distribution of haploblock HB-10–03, which includes the "SNP_FB_0003490", among five biparental populations grouped according to their haplotypes for the Dim1 storage index.

$[2\ln(BF)_{1/0} = 2.6]$ was consistently provided for at least one QTL mapped at the beginning of chromosome 10 (Fig. 6), located in the QTL region defined by the haploblock HB-10–9, which genetic region ranged from 18.00 cM to 44.11 cM with a mode at 28.00 cM. For HB-10–9, 13 haplotypes defined by 20 SNPs were present in the parents of seedling families.

The estimated genotypes (Table 1) of the eight parental cultivars for the QTL identified in the PBA (HB-10–9), were consistent when compared with the Dim1 storage index performance of seedling families (Figures S4 and S5), underlining the impact of the assigned "Q/q" QTL-allelic effects. The haplotypes at chromosome 10 were associated with a QTL for texture retainability. The allelic flow over the founder cultivars (Figure S6) indicated that the founding sources of favorable haplotypes derived from 'Malinda,' 'Greensleves,' 'Duchess of Oldenburg,' and 'Cox Orange Pippin.'

The PBA approach validated chromosome 10 as an important locus controlling the texture attributes in apple. However, the QTL for the Dim1 storage index identified in the GWAS (HB-10–3, Fig. 3), was in a different region than the QTL for the Dim1 storage index (HB-10–9) identified in the PBA (Fig. 6). The HB-10–9 region is, however, corresponding to other QTL regions related to texture. The position of HB-10–9 corresponds to previously identified QTLs for mechanical sub-traits (Di Guardo et al., 2017) and was located 0.71 cM apart from the genetic position of *MdPG1,* a gene known to play a key role in the genetic control of fruit texture (Fig. 7). The PBA results did not provide however strong evidence for QTLs at the end of chromosome 10 for the Dim1 storage index. Although not statistically significant, all acoustic sub-traits detected QTL regions at the end of chromosome 10 (Figure S3), closely mapped to the MdACO1 SNP marker (Fig. 7).

The genotypes of the two haploblocks identified in this study across the parents of seedling families, are depicted in Fig. 7B. All cultivars had one or two copies of the high firmness allele at HB-10–3. Similar results

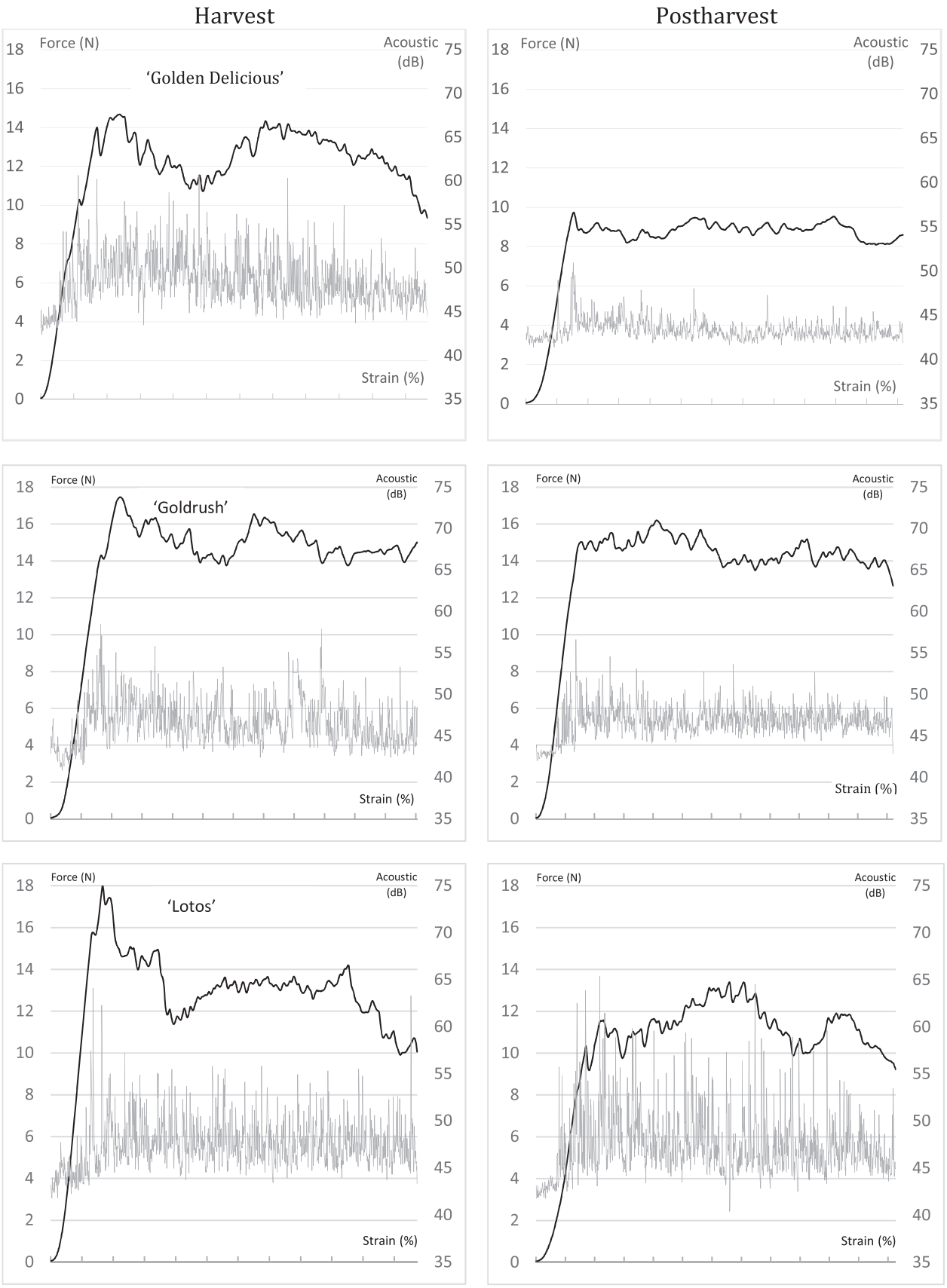

Fig. 4. Texture profiles for cultivars selected as a case to illustrate three typical scenarios of texture dynamics assessed during storage, with profiles at harvest and profiles after storage depicted in the left and right panel, respectively. Acoustic profiles are illustrated with grey lines (dB) and the black lines correspond to the mechanical profile (N), from 0 % to 90 % strain along the X axis.

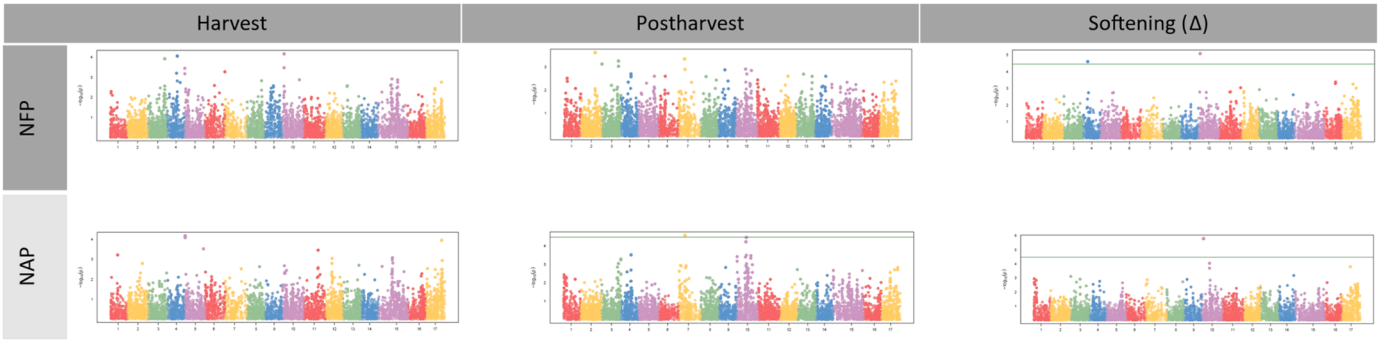

Fig. 5. Manhattan plots using MLMM for harvest, postharvest and for the softening (Δ)index for the sub-traits "force peaks" and "acoustic peaks".

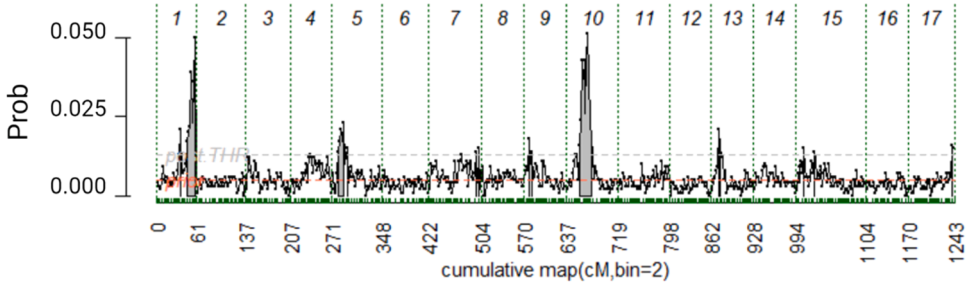

Fig. 6. Posterior QTL positions from FlexQTL for the Dim1 storage index, from a run with five prior QTL, with chromosome numbers, and cumulative genetic distance on the top and bottom row, respectively.

Table 1
Estimated QTL (EQTL) genotypes and estimated breeding value (EBV) for each of the eight parental cultivars at the detected texture retainment QTL. QTL genotypes are recorded as the number of Q alleles present (0 [qq], 1 [Qq], 2 [QQ], inc [inconclusive]) where Q and q are associated with high and low Dim1 storage index values, respectively. The QTL region identified on chromosome 10 as shown in the table is HB-10–9.

	Dim1 storage index					
QTL interval	Chr1		Chr5		Chr10	
Most probable QTL position (mode) cM	60.00		76.00		28.00	
Posterior intensity (probability)	0.21		0.19		0.46	
Posterior intensity (probability)	**EBV**	**EQTL**	**EBV**	**EQTL**	**EBV**	**EQTL**
'Eir'	−0,17	0	−0,01	inc	0,10	2
'Fonn'	−0,12	0	−0,04	0	−0,04	inc
'Gala'	0,00	1	0,02	inc	0,29	2
'Minnewashta'	0,12	2	0,10	2	0,23	2
'NB 2–10'	−0,11	0	−0,02	inc	−0,07	1
'Silva'	−0,13	0	−0,08	0	−0,04	0
'X 4876'	0,13	2	0,10	2	0,25	2
'Tiara'	−0,03	1	−0,01	1	−0,19	0

were reported at HB-10–9, except for two cultivars (Tiara' and 'Silva'), that did not present any copy of the high firmness allele. Among the parental cultivars, only 'Minnewashta' and 'X 4876' had two copies for the favorable firmness alleles at both markers.

3.5. Evaluation of markers related to texture

A significant correlation between harvest date and texture performance was observed. Late-harvested apples had overall better texture performance both at harvest (R2 = 0.46) and after storage (R2 = 0.60), and they also retained texture during storage (R2 = 0.32) (Figure S7). Texture at harvest was also significantly correlated with texture after storage (R2 = 0.58) and texture after storage was significantly correlated with the storage index (Figure S7). The role of six texture-related genetic markers in predicting the texture dissected phenotypic parameters was assessed, and the HB-10–3 marker outperformed the other five for texture retention (Figure S8). Texture at harvest was best predicted by MdACS1 and HB-10–3 when harvest date was considered as a factor (Fig. 8 and Figure S8), while NAC18.1 had the highest predictive power for harvest date across Nordic apple germplasm (Figure S8 and Figure S9). We observed a strong relationship between harvest date on texture performance at harvest, after storage, and for the storage index, accounting for 11.25 %, 24.54 %, and 8.98 % of the variation, respectively (Fig. 8). The amount of phenotypic variance in texture retention explained by HB-10–3 was reduced from 7.69 %, when harvest date was not included in the model (Figure S8), to 5.85 % when harvest date was accounted for (Fig. 8).

4. Discussion

QTLs for multiple texture components assessed at harvest and postharvest together with the softening and the storage indexes were identified across the genome, with chromosome 10 showing however the highest number of associations across the two types of genetic background. An increased magnitude in the association level was detected for the general textural performance (Dim1) computed for the storage index, and associated SNPs were located on the top of chromosome 10.

4.1. Change in texture performance during storage

Phenotypic variation of the fruit texture properties measured among different accessions at harvest, postharvest, and for the softening and storage indexes were presented in this study. The overall texture variability, expressed by Dim1 and Dim2, was between 74.2 % and 86.0 %, depending on the phenotypic time point. These results were consistent with similar studies (Costa et al., 2012; Di Guardo et al., 2017). The effect of the ripening stage was clearly visualized by the comparison of the PCA loading (Figs. 1B and 1 C). Three groups of texture dissected variables were observed at harvest, while after a period of storage, the

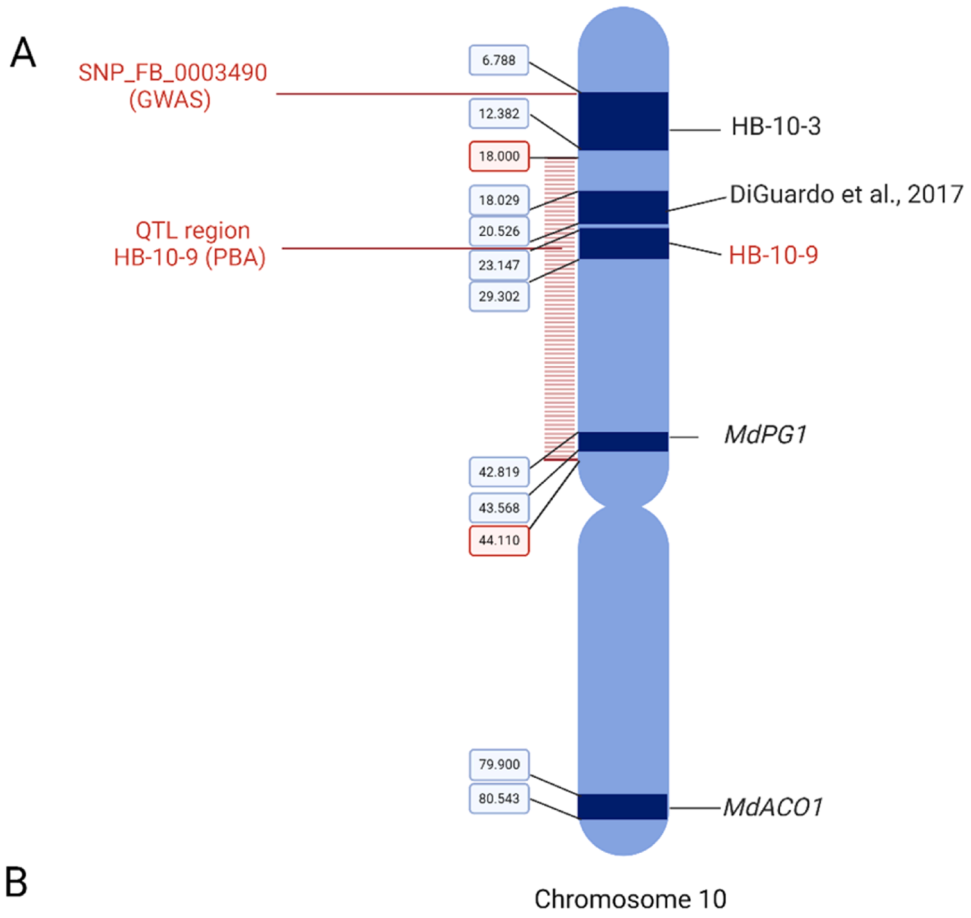

Parents	HB-10-3	HB-10-9
Eir		
Fonn		
Gala		
Tiara		
Silva		
Minnewashta		
X_4876		
NB 2-10		

Genotypes: Homozygot (Undesirable); Heterozygot; Homozygot (Desirable)

Fig. 7. A Genetic markers important for texture on chromosome 10 as identified in this study (marked in red) and in previous studies (Costa et al., 2005; Di Guardo et al., 2017; Longhi et al., 2013). B Genotypes of the texture-related genetic markers HB-10–3 and HB-10–9 across the parents of seedling families. The "desirable" allele for each marker is defined as the allele that has been reported to lead to firmer apple texture.

same variables were clustered in two groups (mechanical and acoustic), underlining that during storage, several processes affecting phenotypic determination of texture occur. This observation is supported by the findings of Costa et al. (2011) and Di Guardo et al. (2017), reporting that fruit softening, related to the cell degradation process, is a cultivar dependent phenomenon underlying a specific genetic control. Similarly, the results of this study suggested that texture at harvest, postharvest and softening are under different genetic control, as indicated by the change in projections of variables (Fig. 1). However, as reported both in this study (Table S5) and in previous works (Di Guardo et al., 2017; Jung et al., 2022), QTLs for different texture attributes are often co-located, indicating pleiotropic effects. A plausible hypothesis is that mechanical and acoustic texture components initially assessed at harvest and then after storage and considering also the dynamic aspect, are mutually related attributes, yet partially independent (Costa, 2014; Wu et al., 2021). The distinctness of the three texture attributes is highlighted by the observed changes in contribution of Dim1 and Dim2 across all PCA plots (Fig. 1). Explained variability for Dim1 was highest at postharvest,

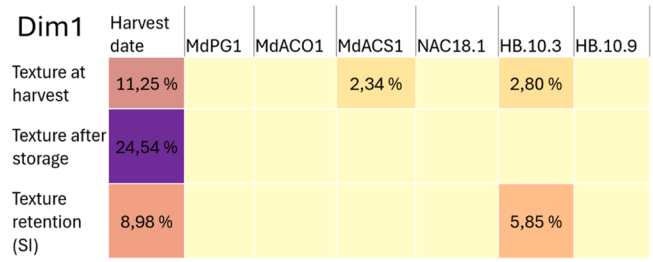

Fig. 8. Prediction of texture related apple phenotypes in diverse Nordic apple germplasm. Six genetic markers including two identified in this study and harvest date were included as factors in a type 2 ANOVA with three different phenotypes as outcomes. The proportion of the variance explained is shown in cases where a statistically significant result ($P < 0.05$) was observed. A type 2 ANOVA was also performed with harvest date as a phenotypic trait (Fig. S8).

consistent with the results of Costa et al. (2012). Meanwhile, for Dim2, slightly more variability was explained for the storage index compared to postharvest. This variation in phenotypic variability could be linked to the observation of differences in texture dynamics among cultivars during storage (Fig. 4). Similarly to Costa et al. (2012), three types of texture profiles were observed (Fig. 4). Popular cultivars in Northern countries, such as 'Summerred' and 'Discovery', showed a general decrease in both mechanical and acoustic profiles from harvest to postharvest. This decrease was as expected, considering they both present a single dose of the HB-10–3 allele associated with loss of texture.

Regardless of the stage of when texture was assessed, the mechanical parameter NFP was grouped in the acoustic parameter subset. This mechanical component has shown to be related to the disruption of each cell of the fruit cortex, a basic event at the base of the release of the sound pressure conferring the properties of crispness (Longhi et al., 2012; Roth et al., 2020). As suggested by Roth et al. (2020), this mechanical trait could in practice replace acoustic traits that are indeed complex to measure, minimizing thereby the phenotyping efforts.

4.2. Temporal QTL dynamics elucidate the genetic control of fruit storability and the role of QTLs on chromosome 10

The results of this study suggest the existence of a QTL dynamic for texture over storage. This hypothesis was supported by the higher magnitude of SNP associations observed for texture components assessed at postharvest or considering storage, compared to those assessed at harvest. Several QTL mapping studies evaluated apple texture at harvest only, such as the case of a *NAC* gene found in apple, *NAC18.1,* and the resulted associations to firmness and maturity date (Jung et al., 2022; Migicovsky et al., 2016). Although effective to select for high firmness, screening for the favorable *NAC18.1* allele would select also late season accessions, not suitable for Nordic growing conditions. The evidence for interdependence between harvest date and fruit firmness has been demonstrated in several studies (Chagné et al., 2014; Jung et al., 2022; Migicovsky et al., 2016). Although fruit texture can vary among cultivars also at harvest (Jung et al., 2022; McKay, 2010), the variability is maximized after a period of storage (Kouassi et al., 2009), as result of the action of cell wall degrading enzymes. This phenomenon is also supported by our findings, where a considerable phenotypic variance in firmness sub-traits at harvest was observed, yet postharvest measurements resulted in higher phenotypic variance, possibly influenced by additional QTLs that impact firmness and crispness maintenance. QTL analyses have traditionally focused on detecting major genes controlling the expected mean of a phenotype. We found that the number of QTLs detected corresponded with the magnitude of phenotypic variability for each specific trait in this study (Fig. 5). This is consistent with the hypothesis from an earlier study (Rönnegård & Valdar, 2011) that not only the mean, but also the variance, may itself be under genetic control.

GWAS and biparental studies have identified several large-effect loci for firmness and firmness retainability on chromosome 10 (Costa et al., 2010; Longhi et al., 2012) with one of the most studied genes being *MdPG1* (Costa, 2014). The two QTLs consistently identified by GWAS and PBA for the overall texture variability in this study, were both mapped on chromosome 10, although not co-locating with *MdPG1*. For the haploblock marker identified by GWAS (HB-10–3), the identified region was co-located with those found for all acoustic sub-traits and YM. It was unexpected, however, that the sub-trait IF did not show any significant associations (Table S5), as it was shown as an important sub trait in previous studies (Di Guardo et al., 2017; Longhi et al., 2012). Although the acoustic and mechanical subsets were oriented towards two different PCA quadrants, they were projected in the same direction along the Dim1 orientation (Fig. 1). The shared projection of the entire group of texture parameters along Dim1, made this a parameter less valuable in the dissection of the genetic control of the acoustic and mechanical texture components. Possibly, the more subtle variability present in the acoustic profile, was overshadowed by the mechanical profile. This theory is supported by the fact that most apple breeding programs have relied on the penetrometer method to assess texture (firmness) rather than acoustic instruments (crispness) (Evans et al., 2010). Consequently, when Dim2 was used as a phenotypic trait, not a single QTL was identified, although this would be more valuable for the selection of apple accessions distinguished by a superior crispness.

A second peak on chromosome 10, as shown in the Manhattan plot, was detected after storage, but with a statistical value below the multiple comparison's threshold. This QTL colocalized with the *MdPG1* gene, one of the most studied elements controlling firmness after storage and softening (Davies & Myles, 2023; Longhi et al., 2012). In this work, the *MdPG1* gene was mapped through the FEM_cg_19 SNP marker (located at 27,287,583 bp), also named MdPG1SNP (Baumgartner et al., 2016), and linked to the microsatellite marker $MdPG1_{SSR}$10kd, previously connected to apple fruit texture properties (Longhi et al., 2013). Moreover, the two QTLs on chromosome 10 as revealed by the Manhattan plots (Fig. 2) suggested the presence of two major QTLs, in agreement with previous studies investigating the genetic control of fruit firmness in apple (Bink et al., 2014). The observation that only one genetic region showed SNPs exceeding the FDR-corrected threshold may be explained by the overly conservative thresholds corrected for multiple comparisons. The MLMM model using the Bonferroni and FDR correction could have been excessively conservative, as it did not identify significant SNPs, whereas the FarmCPU model, which uses less stringent correction factors, did find significant SNPs. FarmCPU model has been previously reported as being more accurate than other GWAS models at identifying the closest number of "true" QTLs (Kaler et al., 2020).

We attempted to validate QTLs initially identified through GWAS using a PBA approach, which employed the simultaneous marker-trait association analysis on five bi-parental families, enabling the detection of several QTLs. For the Dim1 storage index, the QTL on chromosome 10 (HB-10–9) was characterized by an estimated genotype (Table 1) consistent with phenotypic performance of the eight parental cultivars (Figure S5). The estimated QTL genotype "QQ" was the favorable one for the Dim1 storage index, indicating a textural enhancement during storage, and among the parental lines, 'X 4876' ("QQ"), 'Rubinstep' ("QQ") and 'Minnewashta' ("QQ") had the highest texture retention response, as depicted in the PCA plot (Figure S4). In contrast, cultivars with a mealy texture after storage, such as 'Tiara,' were plotted on the opposite quadrant of the PCA plot, showing an unfavorable "qq" genotype for this QTL (Figure S5). All the parental cultivars evaluated in this study, except for 'X 4876,' which had an incomplete pedigree, had the favorable haplotypes inherited from 'Grimes Golden,' 'Duchess of Oldenburg,' 'Cox Orange Pippin,' or 'Malinda' (Figure S6). The seedlings with a favorable homozygous "Q" allele only, and progenies in Fam 5 ('X 4876' x 'Gala') in particular, had a textural enhancement during storage (Figure S5), highlighting the role of this QTL in control of storability in

apple.

The three classes of gene families found near the most significant region highlighted by the GWAS analysis (coinciding with SNP_FB_0003490) and located on chromosome 10 are known to be involved in fundamental aspects of fruit firmness/softening processes and warrants further functional investigation. The first gene was an *endoglucanase*. A similar gene in tomato (*SlCel2*), synergistically acting with a fruit ripening associated *expansin* (ISlExp1), significantly influenced the cell-wall disassembly process, subsequently affecting fruit firmness and softening (Su et al., 2024). These findings might shed light on the role of cellulose-xyloglucan matrix reorganization in fruit softening. The disassembly process of the cellulose-hemicellulose matrix mediated by endoglucanase was also reported as a basic mechanism in fruit softening in strawberry, occurring at the onset of fruit ripening (Jara et al., 2019). The second element was a *xylan alpha-glucuronosyl transferase* that in rice was reported to promote the accumulation of cellulose and hemicellulose, conferring a higher thickness and strength to the cell-wall structure (Gao et al., 2020). The last element was a *cellulose synthase* that is involved in the anabolic phase of the cellulose-hemicellulose structure. Consistent with the catabolic degrading processes involved in fruit ripening in several fleshy fruits, *FveCesA*, a *cellulose synthase* gene, was transcriptionally repressed during the ripening in *Fragaria vesca* (Huang et al., 2022). The regulation of texture characteristics in fruit is governed by amphibolic processes, consisting of both early-biosynthetic and dismantling processes of the cell-wall structure (Brummell & Harpster, 2001).

4.3. Multiple loci implicated in texture and texture retainability

Among the association profiles detected in the present study, those on chromosome 10 were the most significative, but it is also worth noting the identification of associations also on other chromosomes (Table S5 and S7), consistent with the hypothesis that fruit firmness is a complex and multigenic trait (Bink et al., 2014). Both GWAS and PBA showed statistically significant SNP-trait associations on chromosome 1 related to mechanical traits at postharvest, and Dim1 for storage index. SNPs associated with firmness at the end of this chromosome have been previously reported (Chagné et al., 2014; Jung et al., 2022). In this work, associations for both mechanical and acoustic traits at postharvest and for the YM storage index were found also at the end of chromosome 3. The coding region of *NAC18.1* is only ~2 Mb apart from the identified regions for FLD and MXA at postharvest, hence it is very likely that these signals are associated with the *NAC18.1* gene (Figure S10). These results are in line with the findings in Larsen et al. (2019) who reported a sequencing based SNP in the coding region of *NAC18.1* to be associated with harvest date. In addition to this, SNPs associated with mechanical traits were reported by the GWAS results at the beginning of chromosome 5, in agreement with the findings reported in Jung et al. (2022), where a firmness QTL also was identified. In the PBA, both mechanical and acoustic traits for the storage index were also found at the end of chromosome 5, and similar results have been reported for the trait NFP (Di Guardo et al., 2017), and for harvest date (Chagné et al., 2014; Jung et al., 2022), validating the multiple loci involved in the control of this phenomenon (Chagné et al., 2014; Jung et al., 2022; Migicovsky et al., 2016).

4.4. Breeding for texture in Norwegian apples

In this work, we demonstrated that the haplotype HB-10–3 is a stronger predictor for texture, at both harvest and postharvest (Fig. 8, Figure S8, and Figure S9). Moreover, consistent with previous works, the type of texture in apple is also determined by harvest date (Migicovsky et al., 2021; Nybom et al., 2013). To this end, we found that when harvest date was included in the type 2 ANOVA as a factor, it resulted the best predictor for texture at harvest, after storage and for the storage index (Fig. 8). In the context of breeding for texture in Norwegian apples through marker-assisted selection, our results propose that apple texture and storability could be improved by selecting for the HB-10–3 favorable haplotypes. This will provide a better efficiency and precision in the selection process. Besides firmness, storability is a crucial phenotype contributing to the economic success of novel accessions, however it requires the acquisition of the phenotype multiple times during storage. An associated molecular marker will certainly enable a more time-effective breeding for this type of trait. Before employing this as a routine screening tool, additional efforts must be dedicated to shed light on aspects not yet fully elucidated, like the role of harvest date as an efficient factor in predicting storability. The PBA performed on a set of pedigree-related bi-parental populations is evidently a valuable strategy to validate QTLs, for enhanced statistical power and for the possibility offered by this strategy to inspect the effect of minor alleles. However, a new and improved experimental setup with a higher number of individuals is needed, as exemplified by the nondetection of QTLs in the regions of *MdPG1* or *NAC18.1*. Moreover, taking into consideration the complex genetic control of fruit texture, with different loci interacting and QTL profiles changing with regards to the time of phenotyping, other genetic approaches, such as genomic selection, should be employed, to increase the breeding efficiency and genetic gain. In a large multi-environment study, Jung et al. (2022) found that traits such as fruit firmness showed a strong genotypic effect and a comparably low effect of environment and G×E, suggesting that selection for this trait would be efficient when using main-effect genomic prediction models. In conclusion, the new phenotypic method enabling a more informative and precise dissection of the fruit texture, and the availability of markers associated with these parameters can represent a valuable advancement in the improvement of fruit quality and storability in Norwegian apple breeding programs (Brown, 2012; Jung et al., 2022).

Contributions

L.G. and F.C. conceived and designed the research. L.G. collected the samples and measured the fruit traits, N.P.H. and L.G. curated the genotypic data, L.G and F.C. analyzed the data for SNP-trait associations, L.G. wrote the original draft, L.G, F.C, N.P.H., D.R. and M.A. revised the manuscript. All authors approved the final version of the manuscript.

CRediT authorship contribution statement

Liv Gilpin: Writing – review & editing, Writing – original draft, Visualization, Validation, Resources, Project administration, Methodology, Investigation, Funding acquisition, Formal analysis, Data curation, Conceptualization. **Nicholas P. Howard:** Writing – review & editing, Supervision, Data curation. **Fabrizio Costa:** Writing – review & editing, Validation, Supervision, Methodology, Conceptualization. **Muath Alsheikh:** Writing – review & editing, Supervision, Resources, Conceptualization. **Dag Røen:** Writing – review & editing, Supervision, Resources, Funding acquisition.

Declaration of Competing Interest

The authors declare the following financial interests/personal relationships which may be considered as potential competing interests. Liv Gilpin reports financial support was provided by Research Council of Norway. If there are other authors, they declare that they have no known competing financial interests or personal relationships that could have appeared to influence the work reported in this paper.

Acknowledgements

This research was funded by a PhD scholarship from the Research Council of Norway (Project nr. 322,792) and a generous grant from Sparebankstiftinga Sogn og Fjordane. We gratefully acknowledge and thank Michela Troggio at Fondazione Edmund Mach, for facilitating a

research internship and for conducting expertise work at their genomics platform, both of which were instrumental for the accomplishments of this paper. We are grateful to our colleagues Susanne Windju and Espen Sørensen for fruitful discussions and valuable help during data curation and to our colleagues at Graminor and Njøs Fruit and Berry Centre, Susann Herzog, Kurab Røen, Anete Busa, Anne Sigrid Skjerdal, Sigurd Molvik, Sverre Moe, and Wenche Johansen for skillful technical assistance in the laboratory and in the field. The authors gratefully acknowledge and thank Stijn Vanderzande at Wageningen University & Research for facilitating a short research stay and supervising/teaching in the use of the FlexQTL software.

Appendix A. Supporting information

Supplementary data associated with this article can be found in the online version at doi:10.1016/j.postharvbio.2024.113276.

Data availability

Data will be made available on request.

References

Anderson, J.L., Richardson, E.A., Kesner, C.D., 1986. Validation of chill unit and flower bud phenology models for 'Montmorency' sour cherry. Acta Hortic. 184, 71–75.

Baumgartner, I.O., Kellerhals, M., Costa, F., Dondini, L., Pagliarani, G., Gregori, R., Patocchi, A., 2016. Development of SNP-based assays for disease resistance and fruit quality traits in apple (Malus × domestica Borkh.) and validation in breeding pilot studies. Tree Genet. Genomes *12* (3), 35. https://doi.org/10.1007/s11295-016-0994-y.

Benjamini, Y., Hochberg, Y., 1995. Controlling the False Discovery Rate: A Practical and Powerful Approach to Multiple Testing. J. R. Stat. Soc.: Ser. B (Methodol. *57* (1), 289–300. https://doi.org/10.1111/j.2517-6161.1995.tb02031.x.

Bianco, L., Cestaro, A., Sargent, D.J., Banchi, E., Derdak, S., Di Guardo, M., Gut, I., 2014. Development and validation of a 20 K single nucleotide polymorphism (SNP) whole genome genotyping array for apple (Malus× domestica Borkh). PloS One *9* (10), e110377. https://doi.org/10.1371/journal.pone.0110377.

Bink, M.C.A.M., Boer, M.P., ter Braak, C.J.F., Jansen, J., Voorrips, R.E., Van de Weg, W. E., 2008. Bayesian analysis of complex traits in pedigreed plant populations. Euphytica *161* (1), 85–96. https://doi.org/10.1007/s10681-007-9516-1.

Bink, M.C.A.M., Jansen, J., Madduri, M., Voorrips, R.E., Durel, C.E., Kouassi, A.B., van de Weg, W.E., 2014. Bayesian QTL analyses using pedigreed families of an outcrossing species, with application to fruit firmness in apple. Theor. Appl. Genet. *127* (5), 1073–1090. https://doi.org/10.1007/s00122-014-2281-3.

Bowen, A.J., Blake, A., Tureček, J., Amyotte, B., 2019. External preference mapping: A guide for a consumer-driven approach to apple breeding. J. Sens. Stud. *34* (1), e12472. https://doi.org/10.1111/joss.12472.

Brown, S., 2012. Apple. In: Badenes, M.L., Byrne, D.H. (Eds.), Fruit breeding, handbook of plant breeding. Springer-Verlag, pp. 329–367.

Brummell, D.A., Harpster, M.H., 2001. Cell wall metabolism in fruit softening and quality and its manipulation in transgenic plants. Plant Mol. Biol. *47* (1-2), 311–340.

Busatto, N., Farneti, B., Tadiello, A., Velasco, R., Costa, G., Costa, F., 2016. Candidate gene expression profiling reveals a time specific activation among different harvesting dates in 'Golden Delicious' and 'Fuji' apple cultivars. Euphytica *208* (2), 401–413. https://doi.org/10.1007/s10681-015-1621-y.

Chagné, D., Dayatilake, D., Diack, R., Oliver, M., Ireland, H., Watson, A., Tustin, S., 2014. Genetic and environmental control of fruit maturation, dry matter and firmness in apple (Malus× domestica Borkh. Hortic. Res. *1*. https://doi.org/10.1038/hortres.2014.46.

Costa, F., 2014. MetaQTL analysis provides a compendium of genomic loci controlling fruit quality traits in apple. Tree Genet. Genomes *11* (1), 819. https://doi.org/10.1007/s11295-014-0819-9.

Costa, F., Cappellin, L., Fontanari, M., Longhi, S., Guerra, W., Magnago, P., Biasioli, F., 2012. Texture dynamics during postharvest cold storage ripening in apple (Malus×domestica Borkh.). Postharvest Biol. Technol. *69*, 54–63. https://doi.org/10.1016/j.postharvbio.2012.03.003.

Costa, F., Cappellin, L., Longhi, S., Guerra, W., Magnago, P., Porro, D., Gasperi, F., 2011. Assessment of apple (Malus×domestica Borkh.) fruit texture by a combined acoustic-mechanical profiling strategy. Postharvest Biol. Technol. *61* (1), 21–28. https://doi.org/10.1016/j.postharvbio.2011.02.006.

Costa, F., Peace, C.P., Stella, S., Serra, S., Musacchi, S., Bazzani, M., Van de Weg, W.E., 2010. QTL dynamics for fruit firmness and softening around an ethylene-dependent polygalacturonase gene in apple (Malus×domestica Borkh. J. Exp. Bot. *61* (11), 3029–3039. https://doi.org/10.1093/jxb/erq130.

Costa, F., Stella, S., Van de Weg, W.E., Guerra, W., Cecchinel, M., Dallavia, J., Sansavini, S., 2005. Role of the genes Md-ACO1 and Md-ACS1 in ethylene production and shelf life of apple (Malus domestica Borkh). Euphytica *141*, 181–190. https://doi.org/10.1007/s10681-005-6805-4.

Costa, F., Van de Weg, W.E., Stella, S., Dondini, L., Pratesi, D., Musacchi, S., Sansavini, S., 2008. Map position and functional allelic diversity of Md-Exp7, a new putative expansin gene associated with fruit softening in apple (Malus × domestica Borkh.) and pear (Pyrus communis). Tree Genet. Genomes *4* (3), 575–586. https://doi.org/10.1007/s11295-008-0133-5.

Daccord, N., Celton, J.-M., Linsmith, G., Becker, C., Choisne, N., Schijlen, E., Bucher, E., 2017. High-quality de novo assembly of the apple genome and methylome dynamics of early fruit development. Nat. Genet. *49* (7), 1099–1106. https://doi.org/10.1038/ng.3886.

Davies, T., Myles, S., 2023. Pool-seq of diverse apple germplasm reveals candidate loci underlying ripening time, phenolic content, and softening. Fruit. Res. *3* (1). https://doi.org/10.48130/FruRes-2023-0011.

Di Guardo, M., Bink, M.C.A.M., Guerra, W., Letschka, T., Lozano, L., Busatto, N., Costa, F., 2017. Deciphering the genetic control of fruit texture in apple by multiple family-based analysis and genome-wide association. J. Exp. Bot. *68* (7), 1451–1466. https://doi.org/10.1093/jxb/erx017.

Di Pierro, E.A., Gianfranceschi, L., Di Guardo, M., Koehorst-van Putten, H.J.J., Kruisselbrink, J.W., Longhi, S., van de Weg, W.E., 2016. A high-density, multi-parental SNP genetic map on apple validates a new mapping approach for outcrossing species. Hortic. Res. *3*. https://doi.org/10.1038/hortres.2016.57.

El-Ramady, H.R., Domokos-Szabolcsy, É., Abdalla, N.A., Taha, H.S., Fári, M., 2015. Postharvest Management of Fruits and Vegetables Storage. In: Lichtfouse, In.E. (Ed.), Sustainable Agriculture Reviews, *Volume 15*. Springer International Publishing, pp. 65–152. https://doi.org/10.1007/978-3-319-09132-7_2.

Evans, K., Brutcher, L., Konishi, B., Barritt, B., 2010. Correlation of Sensory Analysis with Physical Textural Data from a Computerized Penetrometer in the Washington State University Apple Breeding Program. HortTechnology hortte *20* (6), 1026–1029. https://doi.org/10.21273/HORTSCI.20.6.1026.

Farneti, B., Di Guardo, M., Khomenko, I., Cappellin, L., Biasioli, F., Velasco, R., Costa, F., 2017. Genome-wide association study unravels the genetic control of the apple volatilome and its interplay with fruit texture. J. Exp. Bot. *68* (7), 1467–1478. https://doi.org/10.1093/jxb/erx018.

Galvez-Lopez, D., Laurens, F., Quéméner, B., Lahaye, M., 2011. Variability of cell wall polysaccharides composition and hemicellulose enzymatic profile in an apple progeny. Int. J. Biol. Macromol. *49* (5), 1104–1109. https://doi.org/10.1016/j.ijbiomac.2011.09.007.

Gilpin, L., Røen, D., Schubert, M., Davik, J., Rumpunen, K., Gardli, K.A., Alsheikh, M., 2023. Genetic Characterization of the Norwegian Apple Collection. Horticulturae *9* (5), 575. https://doi.org/10.3390/horticulturae9050575.

Harrell Jr, F.E., Harrell Jr, M.F.E., 2019. Package 'hmisc'. CRAN2018 *2019*, 235–236.

Holm, S., 1979. A simple sequentially rejective multiple test procedure. Scand. J. Stat. 65–70.

Howard, N.P., Troggio, M., Durel, C.-E., Muranty, H., Denancé, C., Bianco, L., van de Weg, E., 2021. Integration of Infinium and Axiom SNP array data in the outcrossing species Malus × domestica and causes for seemingly incompatible calls. BMC Genom. *22* (1), 246. https://doi.org/10.1186/s12864-021-07565-7.

Howard, N.P., van de Weg, E., Bedford, D.S., Peace, C.P., Vanderzande, S., Clark, M.D., Luby, J.J., 2017. Elucidation of the 'Honeycrisp' pedigree through haplotype analysis with a multi-family integrated SNP linkage map and a large apple (Malus×domestica) pedigree-connected SNP data set. Hortic. Res. *4*. https://doi.org/10.1038/hortres.2017.3.

Huang, H., Zhao, S., Chen, J., Li, T., Guo, G., Xu, M., Su, Y., 2022. Genome-wide identification and functional analysis of Cellulose synthase gene superfamily in Fragaria vesca. Front. Plant Sci. *13*, 1044029. https://doi.org/10.3389/fpls.2022.1044029.

Ikase, L., 2015. Results of fruit breeding in Baltic and Nordic states. Proceedings of 25th Congress of the Nordic Association of Agricultural Scientists (NJF) Nordic View to Sustainable Rural Development, Riga, Latvia.

Jara, K., Castro, R.I., Ramos, P., Parra-Palma, C., Valenzuela-Riffo, F., Morales-Quintana, L., 2019. Molecular insights into FaEG1, a strawberry endoglucanase enzyme expressed during strawberry fruit ripening. Plants *8* (6), 140.

Jung, M., Keller, B., Roth, M., Aranzana, M.J., Auwerkerken, A., Guerra, W., Rymenants, M., 2022. Genetic architecture and genomic predictive ability of apple quantitative traits across environments. uhac028 Hortic. Res. *9*. https://doi.org/10.1093/hr/uhac273.

Jung, S., Lee, T., Cheng, C.H., Buble, K., Zheng, P., Yu, J., Main, D., 2019. 15 years of GDR: New data and functionality in the Genome Database for Rosaceae. D1137-d1145 Nucleic Acids Res *47* (D1). https://doi.org/10.1093/nar/gky1000.

Kaler, A.S., Gillman, J.D., Beissinger, T., Purcell, L.C., 2020. Comparing Different Statistical Models and Multiple Testing Corrections for Association Mapping in Soybean and Maize [Original Research]. Front. Plant Sci. *10*. https://doi.org/10.3389/fpls.2019.01794.

Kass, R.E., Raftery, A.E., 1995. Bayes Factors. J. Am. Stat. Assoc. *90* (430), 773–795. https://doi.org/10.1080/01621459.1995.10476572.

Kassambara, A., Mundt, F., 2017. Package 'factoextra'. Extr. Vis. Results Multivar. data Anal. *76*.

Kouassi, A.B., Durel, C.-E., Costa, F., Tartarini, S., van de Weg, E., Evans, K., Laurens, F., 2009. Estimation of genetic parameters and prediction of breeding values for apple fruit-quality traits using pedigreed plant material in Europe. Tree Genet. Genomes *5* (4), 659–672. https://doi.org/10.1007/s11295-009-0217-x.

Larsen, B., Migicovsky, Z., Jeppesen, A.A., Gardner, K.M., Toldam-Andersen, T.B., Myles, S., Pedersen, C., 2019. Genome-Wide Association Studies in Apple Reveal Loci for Aroma Volatiles, Sugar Composition, and Harvest Date. Plant Genome *12* (2), 180104. https://doi.org/10.3835/plantgenome2018.12.0104.

Laurens, F., Aranzana, M.J., Arus, P., Bassi, D., Bink, M., Bonany, J., van de Weg, E., 2018. An integrated approach for increasing breeding efficiency in apple and peach in Europe. Hortic. Res. *5* (1), 11. https://doi.org/10.1038/s41438-018-0016-3.

Longhi, S., Hamblin, M.T., Trainotti, L., Peace, C.P., Velasco, R., Costa, F., 2013. A candidate gene based approach validates Md-PG1 as the main responsible for a QTL impacting fruit texture in apple (Malus x domesticaBorkh). BMC Plant Biol. *13* (1), 37. https://doi.org/10.1186/1471-2229-13-37.

Longhi, S., Moretto, M., Viola, R., Velasco, R., Costa, F., 2012. Comprehensive QTL mapping survey dissects the complex fruit texture physiology in apple (Malus x domestica Borkh.). J. Exp. Bot. *63* (3), 1107–1121. https://doi.org/10.1093/jxb/err326.

McKay, S.J., 2010. The genetic dissection of fruit texture traits in the apple cultivar honeycrisp. University Of Minnesota], Minneapolis, Minnesota. ⟨https://hdl.handle.net/11299/100651⟩.

Migicovsky, Z., Gardner, K.M., Money, D., Sawler, J., Bloom, J.S., Moffett, P., Myles, S., 2016. Genome to Phenome Mapping in Apple Using Historical Data. plantgenome2015.2011.0113 Plant Genome *9* (2). https://doi.org/10.3835/plantgenome2015.11.0113.

Migicovsky, Z., Yeats, T.H., Watts, S., Song, J., Forney, C.F., Burgher-MacLellan, K., Myles, S., 2021. Apple Ripening Is Controlled by a NAC Transcription Factor [Original Research]. Front. Genet. *12*. https://doi.org/10.3389/fgene.2021.671300.

Nybom, H., 2023. Advances in understanding texture development in apples. In: Costa, F. (Ed.), Improving the quality of apples, Vol. 142. Burleigh Dodds Science Publishing Limited, p. 230. https://doi.org/10.19103/AS.2023.0127.03.

Nybom, H., Ahmadi-Afzadi, M., Garkava-Gustavsson, L., Sehic, J., Tahir, I., 2010. Selection for improved fruit texture and storability in apple. XXVIII International Horticultural Congress on Science and Horticulture for People (IHC2010). International Symposium Leuven, Belgium.

Nybom, H., Ahmadi-Afzadi, M., Sehic, J., Hertog, M., 2013. DNA marker-assisted evaluation of fruit firmness at harvest and post-harvest fruit softening in a diverse apple germplasm. Tree Genet. Genomes *9* (1), 279–290. https://doi.org/10.1007/s11295-012-0554-z.

OFG. (2024). *Frukt- og grøntstatistikk 2023*. Opplysningskontoret for frukt og grønt. ⟨www.frukt.no⟩.

Oye, I., 1998. In: Museum, B. (Ed.), Middelalderbyenes agrare trekk, pp. 7–75.

R Core Team. (2023). *R: A Language and Environment for Statistical Computing*. In (Version 4.3.0) R Foundation for Statistical Computing. ⟨https://www.R-project.org/⟩.

Roth, M., Muranty, H., Di Guardo, M., Guerra, W., Patocchi, A., Costa, F., 2020. Genomic prediction of fruit texture and training population optimization towards the application of genomic selection in apple. Hortic. Res. *7*. https://doi.org/10.1038/s41438-020-00370-5.

Rönnegård, L., Valdar, W., 2011. Detecting Major Genetic Loci Controlling Phenotypic Variability in Experimental Crosses. Genetics *188* (2), 435–447. https://doi.org/10.1534/genetics.111.127068.

Sillanpää, M.J., Arjas, E., 1999. Bayesian mapping of multiple quantitative trait loci from incomplete outbred offspring data. Genetics *151* (4), 1605–1619. https://doi.org/10.1093/genetics/151.4.1605.

Sorensen, D., Gianola, D., 2002. Likelihood, Bayesian, and MCMC Methods in Quantitative Genetics. Springer Science and Business Media. https://doi.org/10.1007/b98952.

Su, G., Lin, Y., Wang, C., Lu, J., Liu, Z., He, Z., Li, B., 2024. Expansin SlExp1 and endoglucanase SlCel2 synergistically promote fruit softening and cell wall disassembly in tomato. Plant Cell *36* (3), 709–726. https://doi.org/10.1093/plcell/koad291.

Vanderzande, S., Howard, N.P., Cai, L., Da Silva Linge, C., Antanaviciute, L., Bink, M.C., Lezzoni, A., 2019. High-quality, genome-wide SNP genotypic data for pedigreed germplasm of the diploid outbreeding species apple, peach, and sweet cherry through a common workflow. PloS One *14* (6), e0210928. https://doi.org/10.1371/journal.pone.0210928.

Voorrips, R.E., Bink, M.C.A.M., Kruisselbrink, J.W., Koehorst Van Putten, H.J.J., Van de Weg, E., 2016. PediHaplotyper: software for consistent assignment of marker haplotypes in pedigrees. Mol. Breed. *36* (8), 119. https://doi.org/10.1007/s11032-016-0539-y.

Wang, J., Zhang, Z., 2021. GAPIT Version 3: Boosting Power and Accuracy for Genomic Association and Prediction. Genom., Proteom. Bioinforma. *19* (4), 629–640. https://doi.org/10.1016/j.gpb.2021.08.005.

Weisberg, J.F. a S. (2019). *An (R) Companion to Applied Regression*. In Sage. ⟨https://socialsciences.mcmaster.ca/jfox/Books/Companion/⟩.

Wickham, H. (2016). *ggplot2: Elegant Graphics for Data Analysis*. In Springer-Verlag New York. ⟨https://ggplot2.tidyverse.org⟩.

Wu, B., Shen, F., Wang, X., Zheng, W.Y., Xiao, C., Deng, Y., Zhong Zhang, X., 2021. Role of MdERF3 and MdERF118 natural variations in apple flesh firmness/crispness retainability and development of QTL-based genomics-assisted prediction. Plant Biotechnol. J. *19* (5), 1022–1037. https://doi.org/10.1111/pbi.13527.